THE JOURNAL OF PHYSICAL CHEMISTRY Letters

Letter

pubs.acs.org/JPCL

Coupling between a Molecular Charge-Transfer Exciton and Surface Plasmons in a Nanostructured Metal Grating

Natalia Azarova,[†] Andrew J. Ferguson,[‡] Jao van de Lagemaat,[‡] Elisabeth Rengnath,[†] Wounjhang Park,[†] and Justin C. Johnson*[,‡]

[†]Department of Electrical, Computer and Energy Engineering, University of Colorado, Boulder, Colorado 80309, United States

[‡]National Renewable Energy Laboratory, 15013 Denver West Parkway, Golden, Colorado 80401, United States

Supporting Information

ABSTRACT: The interaction of molecular excitons in organic thin films with surface plasmon polaritons (SPPs) in nanostructured metal electrodes represents a unique opportunity for enhancing the properties of the active layer of a photoconversion device. We present evidence of hybridization between charge-transfer excitons (CTEs) in 3,4,9,10-perylenetetracarboxylic dianhydride (PTCDA) and SPP modes in silver grating nanostructures. Molecular and SPP absorption peaks exhibit avoided crossings in angle-dependent reflectivity experiments, which are verified by electromagnetic-field simulations of the PTCDA-grating structure. Photoluminescence measurements indicate that the radiative decay of the CTE is enhanced. Besides energetic resonance, selective coupling between the SPP and the exciton in this unique case may be aided by the oriented nature of PTCDA into 1-D "molecular stacks" as well as the delocalized nature of the CTE.

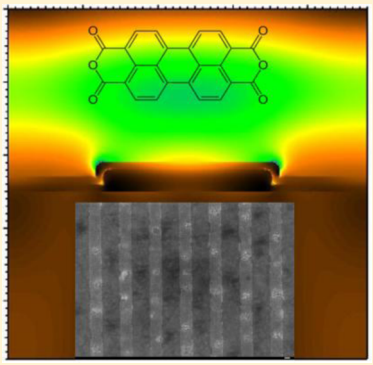

SECTION: Plasmonics, Optical Materials, and Hard Matter

Charge-transfer excitons (CTEs) in molecular systems are often thought of as weakly absorbing and tightly bound species but are potentially important in a variety of contexts where photoinduced electron transfer is a key step in the generation of a desired final state/species in a photophysical scheme (such as solar energy conversion): (i) sub-band gap absorbers;[1] (ii) precursors to free charge carriers;[1,2] and (iii) intermediates in excited state processes.[3−5] In this context, the perylenetetracarboxylic acid derivatives, such as 3,4,9,10-perylenetetracarboxylic dianhydride (PTCDA), which have been studied for optoelectronic device applications, are an interesting class of organic semiconductor.[6−8] The rigid, planar structure of the PCTDA molecules means that they have a propensity to π-stack to form quasi-1D crystals. Theoretical studies have indicated that there are contributions to the absorption spectrum from a Frenkel exciton (FE) and CTE and that the CTE "borrows" oscillator strength from the FE due to mixing of the states,[9] thereby explaining the presence of the low-energy absorption band,[10,11] polarization-dependent absorption, and electroabsorption data.[10] Data acquired using steady-state and time-resolved photoluminescence (PL) spectroscopic techniques have been attributed to emission from an array of excited state species, including FE, CTE, and excimers.[11,12−14] It should be noted that in many cases there have been arguments for the contribution from multiple, distinct states of the same character, mixed states, and even self-trapped CTEs, illustrating the complexity of the excited state decay of PTCDA.

Depending on the specific growth conditions, two very similar crystal polymorphs (both crystallizing in the monoclinic $P2_1/c$ space group) of PTCDA are known to exist, α and β, with molecules in neighboring 1D stacks adopting a herringbone arrangement in both cases, with their long molecular axes essentially orthogonal.[15] Recent studies have indicated that only the α-polymorph exists in vapor-deposited polycrystalline thin films deposited onto quartz via thermal evaporation.[11,16] Structural studies, using X-ray diffraction, of PTCDA films deposited onto Si(100) and quartz reveal a single diffraction peak from the (102) plane of the α-polymorph at 2θ = 27.7° ($d_{102} \approx$ 3.22 Å), indicating that the molecules are oriented approximately parallel (tilted between 10 and 15°) to the substrate surface.[11,15,17] An optical transition with pure CT character will then have a transition moment oriented nearly perpendicular to the substrate.

Surface plasmon polaritons (SPPs) are collective charge oscillations at a metal/dielectric interface that can be thought of as trapped electromagnetic waves. These quasiparticles can, under certain circumstances, hybridize with excitonic energy levels of molecular[18] or nanoscale species such as quantum dots.[19,20] Large Rabi splittings on the order of hundreds of millielectronvolts have been observed in such systems. Usually the hybridization has been studied in the Kretschmann configuration using a metal layer deposited on a prism or

Received: June 12, 2013
Accepted: July 24, 2013

   dx.doi.org/10.1021/jz401219s | J. Phys. Chem. Lett. 2013, 4, 2658−2663

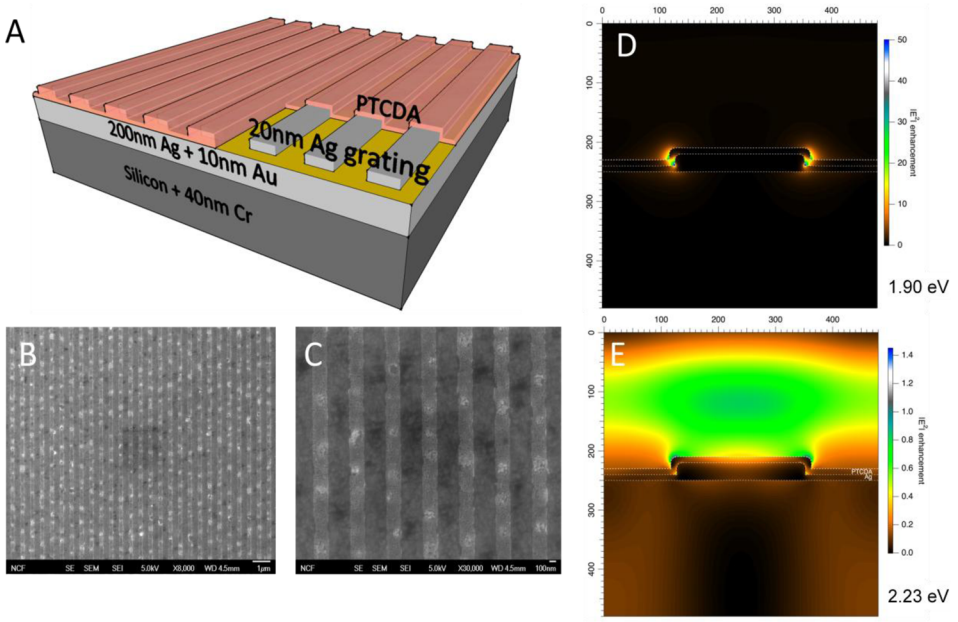

Figure 1. (A) Diagram of sample geometry. (B,C) SEM images of Ag gratings on Si. (D,E) FDTD simulations of the EM field distribution on the grating resonance (1.90 eV (D)) and off resonance (2.23 eV (E)) for the grating structure with PTCDA present. Scales are in nanometers.

hemispherical substrate. Alternatively, in some nanostructured metal architectures, SPPs produce narrow resonances tunable over the visible and near-infrared spectrum, overlapping with conventional solar light absorbers. However, not many of these architectures can be fabricated with high throughput, on an arbitrary substrate, and over large physical areas. Nanostructured "gratings" are actively studied in solar cells,[21] and their ease of fabrication by the inexpensive and scalable nanoimprint lithography technique has made them a natural choice for our investigations, which are fundamental in nature but keep an eye toward eventual practical utilization.

A schematic of the structures used in our experiments is shown in Figure 1A. In brief, a 200 nm thick Ag film was deposited onto a one inch square Si wafer. Glass or ITO was also used, but for fundamental studies the reproducibility of the imprint was found to be superior on Si. Then, a 165 nm thick poly(methyl methacrylate) (PMMA) was spin-coated and the grating pattern was imprinted using a Si mold with an area of 0.66 cm^2. The average dimensions of the grating features made from the mold were 20 nm in height, 237 ± 11 nm wide, with a 493 ± 6 nm pitch, varying by about 5% between individual gratings. Any residual PMMA within the trenches was removed by a carefully controlled oxygen reactive ion etching (RIE) step. To prevent any oxidation of Ag during the RIE process, a 10 nm thick gold layer was deposited on top of silver before PMMA spin-coating. After imprinting, the PMMA pattern was transferred to the Ag grating pattern by evaporation of a 20 nm thick Ag film, followed by lift-off. As shown in the scanning electron micrographs in Figure 1B,C a highly uniform nanograting structure was obtained. The polycrystalline nature of the PTCDA film naturally leads to considerable roughness of the PTCDA layer, although in atomic force microscopy images the underlying grating features are easily discernible, suggesting the depiction in Figure 1A is qualitatively correct. Atomic layer deposition (ALD) of an intervening Al_2O_3 layer was used to avoid direct contact of the PTCDA molecules with metal and to test the distance dependence of the SPP/exciton coupling. However, no significant difference in peak shifting or fluorescence was observed between samples with a thin (2−5 nm) Al_2O_3 layer and no layer. The 50 nm Al_2O_3 interlayers degraded the SPP resonances and removed all evidence of SPP/exciton coupling.

Figure 1D,E shows calculated EM field enhancements for a 10 nm coating of PTCDA on a 479 nm period grating with 226 nm wide and 20 nm thick silver lines on a 10 nm thick silver backing, similar to features from a grating used in experiments described below. The grating lines have rounded corners with a radius of 5 nm to avoid unrealistic sharp corners; however, the true polycrystalline and rough nature of the gratings and the PTCDA layers cannot be fully captured in the simulations. Calculations were performed with the Meep open-source package[22] using a Lorentzian oscillator model for PTCDA, as described in the literature.[23] For the silver dielectric function, a Lorentzian oscillator model including a Drude contribution was fitted to the experimental silver dielectric function[24] to closely approximate the real function at optical wavelengths. All simulations in this study were performed on the NREL red rock cluster using 0.5 nm resolution. It is well-known that the dielectric function of silver changes for nanoscale-sized structures, but we did not attempt to model this. Figure 1D shows the field enhancement at the calculated main grating resonance at 1.9 eV. This wavelength is below the first exciton energy of PTCDA used in the model and therefore represents strongly enhanced sub-"bandgap" absorption. In Figure 1E, the situation at 2.23 eV is shown, illustrating that outside of the resonances the silver backing operates mostly like a mirror. (The same is true for thicker Ag backing.)

The shifts of the resonance peaks of the isolated and combined systems were investigated by a home-built polarization-controlled and angle-resolved reflectance instrument. A Xe lamp was used as the light source, which was either p- or s-polarized with respect to the tilting substrate by use of a beam-splitting cube. The polarized light probed a 3 mm circular region of the sample, which was rotated from 1 to 11° between the sample normal and the incoming beam by a computer-controlled stage. A large Ag focusing mirror collected the

dx.doi.org/10.1021/jz401219s | J. Phys. Chem. Lett. 2013, 4, 2658−2663

reflected light into a liquid light guide, which was aligned to a monochromator and a cooled CCD. A reference scan (bare Ag with no grating or PTCDA) was taken for each angle and polarization. The sample/reference signals were collected for both polarizations, and the p-polarized signal was divided by the s-polarized signal. (Only p-polarized light excites the SPP modes in this configuration.) The resulting data are free from sample-related artifacts due to angle-dependent absorption or scattering from the Ag backing. The SPP modes excited by p-polarized light are expected to couple most strongly to molecular transitions directed out of the substrate plane.

The grating, without any overcoating of organic material, exhibits a single resonance at normal incidence (2.2 eV) that splits into two opposite-moving peaks as the incident angle is increased (Figure 2A). To model the angular dependence of

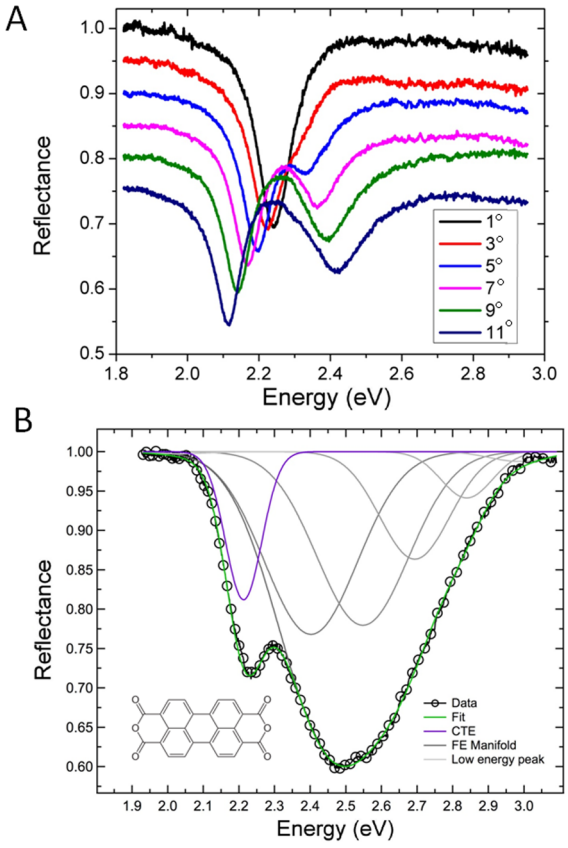

Figure 2. (A) Grating reflectance spectra versus incident angle. (B) PTCDA on flat Ag thin film reflectance spectrum (black circles), fit (green), and underlying fit components. Shades of gray, LE and FE vibronic bands; purple, CTE band.

the grating resonance response, the positions of the individual Gaussian peaks were constrained so that the "splitting" energy (or shift) had a linear dependence on the incident angle (1 to 1.5 meV/degree). The resonances shift to lower energies when a dielectric (either Al_2O_3 or PTCDA) is deposited onto the Ag grating.

PTCDA was deposited using thermal evaporation, and the film thickness and structure/texture were characterized using profilometry, XRD, and UV/vis absorption. For spectroscopic studies, very thin layers (~10 nm) were deposited on the grating structures (Figure 1A) or on an identical substrate but without the grating features. In the absence of the grating features the absorption of PTCDA (Figure 2B), the shape of which is independent of incident beam angle over the range of interest in this study, has peaks attributed to both CT-dominated and FE transitions. The broadband ~2.6 eV mixed CT−FE electronic transition is a vibronic progression of five subbands, where the spectral weight of the individual vibrational bands can be calculated using a Franck−Condon progression, described by a Huang−Rhys parameter. Each subband of the vibrational manifold is represented by a normalized symmetric Gaussian line shape, separated by a vibrational quanta $\hbar\omega$ of ~140 meV, as observed in solution PTCDA.[1,2] The peak at 2.25 eV (CT-dominated state) as well as lower energy peaks around 2 eV are modeled as purely electronic transitions and are also represented by symmetrical Gaussian lineshapes. The sloping background observed in the raw experimental reflectivity data (Figure S6 in the Supporting Information), most likely caused by Rayleigh scattering, has a λ^{-4} dependence that was subtracted from the data shown in Figures 2 and 3.

Reflectivity data were collected on a series of nearly identical gratings, and representative spectra for two angles are displayed in Figure 3, with the components of the photophysical model also included. To model the angle-dependent reflectivity spectra for the grating/Al_2O_3(2−5 nm)/PTCDA sample, the

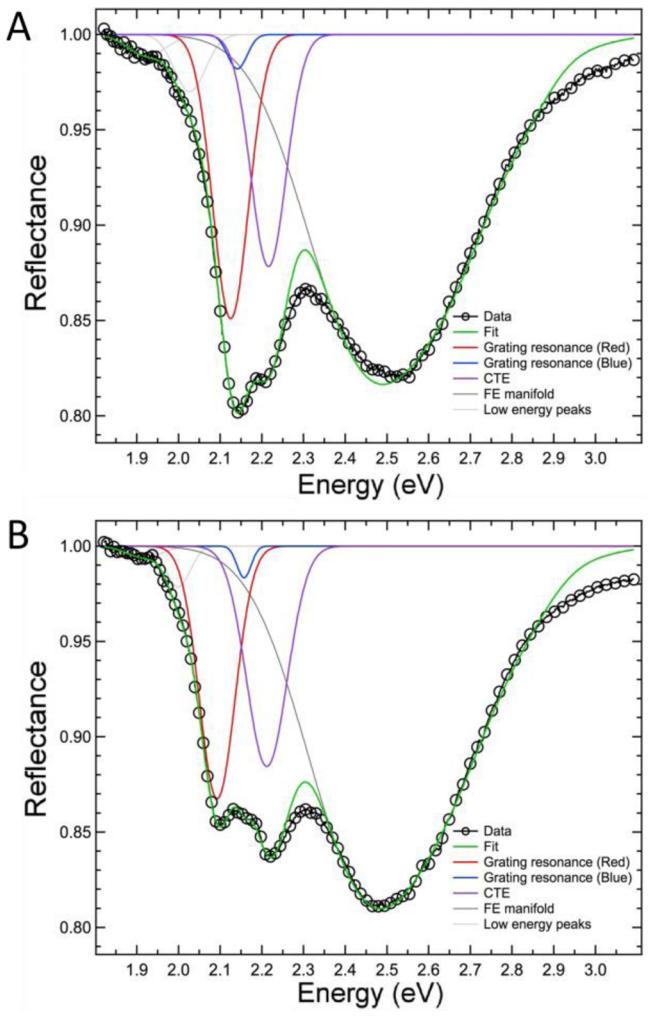

Figure 3. PTCDA/grating reflectance spectra (black circles), fit (green), and underlying PTCDA fit (gray, purple) at (A) 1° and (B) 6° incident angle. Red, lower energy SPP; blue, higher energy SPP.

dx.doi.org/10.1021/jz401219s | J. Phys. Chem. Lett. 2013, 4, 2658−2663

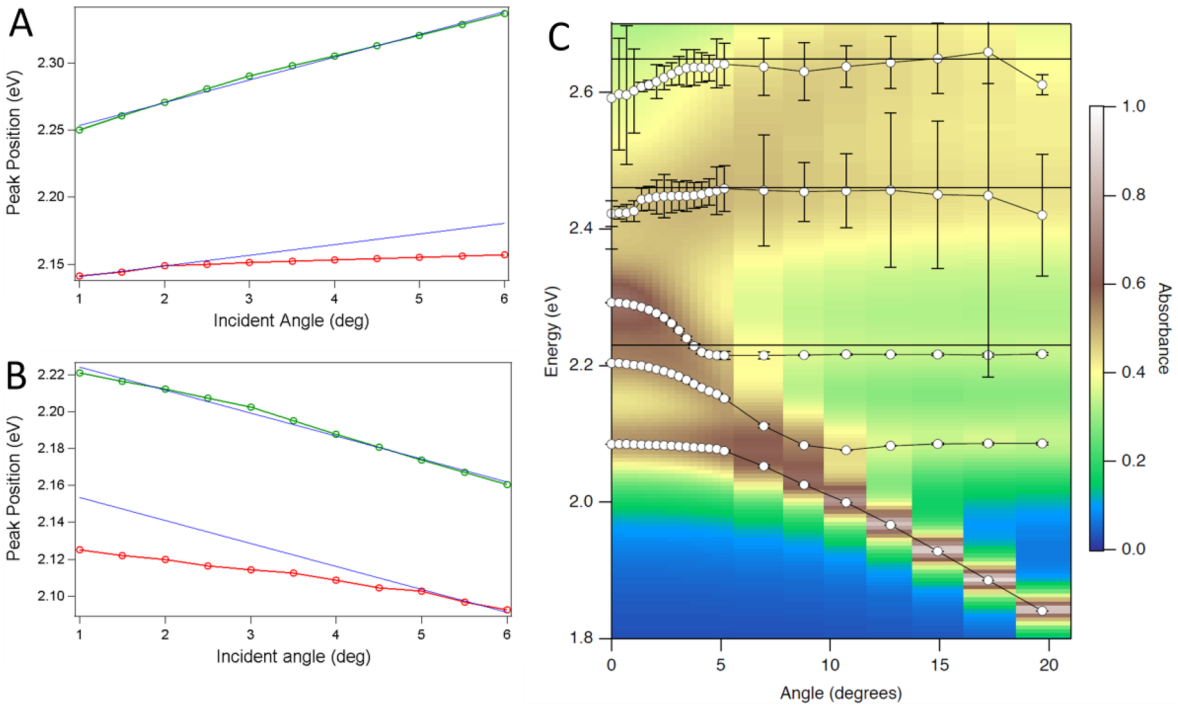

Figure 4. Results of peak fitting for (A) higher and (B) lower energy SPP grating peak for bare grating (green) and PTCDA/2−5 nm Al_2O_3/grating (red). Blue lines are linear fits for the peak position versus angle for bare grating, which are shifted to lower energy for comparison with the PTCDA/Al_2O_3/grating sample. (C) FDTD-simulated peak position versus angle for PTCDA/grating samples described in text.

features attributed to the mixed CTE-FE vibronic progression were essentially kept constant, with only subtle changes to the relative intensities of the individual subbands. As a function of angle, the positions and amplitudes of the peaks due to the Ag grating and CTE-dominated low-energy peak were modified to give the best fit to the low-energy reflectivity features (evaluated visually and by the magnitude of the least-squares error, χ^2). It should be noted that the amplitude of the blue-shifting (hypsochromic) SPP is significantly reduced compared with the bare grating, most likely due to absorption of the incident light by the PTCDA overlayer.

Figure 4 displays the peak positions of the SPP peaks versus incident angle for both bare grating and the grating/2−5 nm Al_2O_3/PTCDA combination. All PTCDA peaks (including the CTE peak) did not change with angle to within experimental uncertainty. On the composite sample at large incident angles the slope of the red-shifting (bathochromic) SPP peak versus angle roughly matches that of the bare grating, but significant deviation is found as the angle decreases. This avoided crossing behavior is similar to that observed in classic exciton/SPP "hybridization," indicating the approach of coupling as the angle brings the SPP into resonance with the static exciton band.[25] The exact opposite behavior versus angle is observed for the blue SPP peak. Because at low angle the red and blue SPPs are both at lower energy than the CTE peak and move away from each other with increasing angle, their opposite anticrossing behavior is evidence that each is coupled to the CTE band. Similar behavior is observed in the absence of the Al_2O_3 layer (Figure S8 in the Supporting Information).

FDTD simulations of the grating structure predict very similar behavior as the angle of the incident light is changed. Figure 4C shows the result of FDTD simulations of a 10 nm thick conformal PTCDA model film on a 479 nm period grating with 226 nm wide lines 20 nm thick having rounded corners with radius of 5 nm. The color scale indicates absorbance. The symbols show peak positions as determined from fitting a series of Lorentzian peaks to the calculated absorption spectra (Figure S1 in the Supporting Information). The horizontal lines show the positions of the excitonic states in PTCDA used as input into the model, derived from ellipsometry studies of thin PTCDA films on glass.[23] The peaks are not identical to those determined from reflectivity experiments on our samples, which leads to uncertainty that cannot be fully avoided because the grating inevitably produces scattering that makes fitting reflectivity data more difficult. Nevertheless, a clear avoided crossing behavior is observed between the peak that starts out at 2.08 eV at zero angle and that at 2.2 eV that is static. This is similar to the behavior of the lower energy SPP peak and the CTE band from experiment (Figure 4B). A second avoided crossing is observed between the peaks at 2.2 and 2.29 that straddle the first PTCDA excitonic state. These two peaks are observed as only one CTE peak at 2.23 eV experimentally due to broadening but are probably both partially hybridized with the SPP. Note that a higher energy SPP peak that increases in energy versus angle is not directly observed in the simulation, which may be due to strong attenuation of this mode as it is confined near the metal surface and travels through an effectively large path length of PTCDA. Under experimental conditions this peak is also attenuated, although disorder and scattering may reduce the degree of attenuation compared with the simulation.

The coupling between the SPP and CTE bands observed in the reflectivity data, combined with the close proximity of the photogenerated excitons to the metal grating, suggests that an enhanced radiative decay rate may be expected owing to the well-known Purcell effect.[26] PTCDA is not an ideal system for investigating altered decay kinetics because the PTCDA fluorescence is relatively complex and involves at least three

dx.doi.org/10.1021/jz401219s | J. Phys. Chem. Lett. 2013, 4, 2658−2663

exponential decay components,[11,12,13] and we found a satisfactory fit with either four or five decay constants. However, the dominant rate constants ranging from ~3 to a 0.3 ns^{-1} are consistently larger for fluorescence collected from PTCDA on the grating compared with decays measured on the same sample but at a position with no grating features where only flat silver backing is present (Figure 5B). For example, for

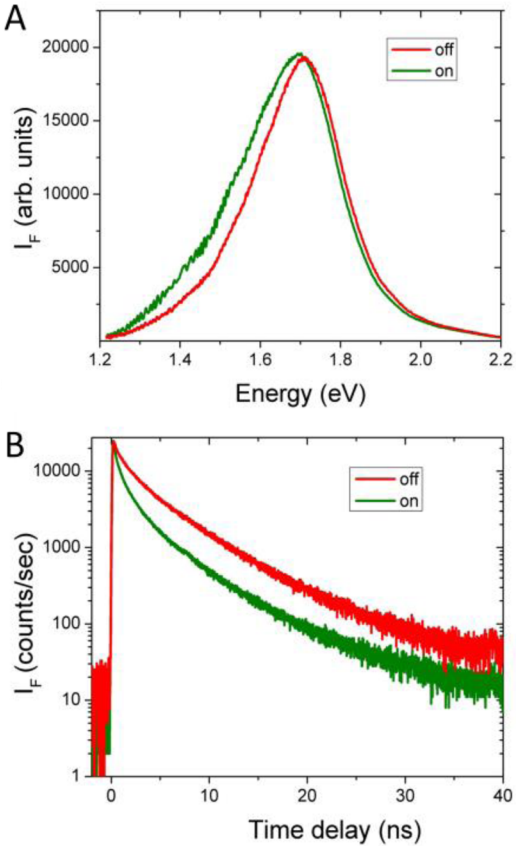

Figure 5. (A) Steady-state and (B) time-resolved photoluminescence collected at 1.45 eV of PTCDA/metal samples either on or off the region with grating features.

the data shown in Figure 5B, the average fluorescence lifetime for PTCDA on the grating was 668 ps, while off the grating it was 921 ps. The average lifetime was used because it was not possible to clearly separate the change of each individual rate constant due to covariance. Although this lifetime varied somewhat on different samples, on average it decreased by 25% on the grating versus off. This is a rather small enhancement compared with expectations for strong coupling, which may be because at room temperature most of the emission occurs from electronic states that do not couple to the SPP (i.e., FEs or excimers), whereas the CTE states have a lower contribution.[12] In addition, for molecules that are in contact with the metal surface, the increased rate could result from enhanced nonradiative decay due to well-known molecule-metal quenching.[27] However, the simultaneous observation of increased PL decay rate and increased emission intensity in the low-energy spectral region 1.3 to 1.7 eV (Figure 5A) suggests that at least some CTEs undergo true radiative decay rate enhancement. While adding the intervening 2−5 nm Al_2O_3 layer produced results similar to Figure 5, measurements in which a 50 nm Al_2O_3 spacer was included exhibited decays that were similar to within 10% on versus off grating, and no change in the spectrum was observed (Figure S3 in the Supporting Information). While a measure of the true radiative rate, involving an accurate measurement of the fluorescence quantum yield, was not possible due to the nature of the sample and underlying substrate, the change in spectral shape combined with the altered rate constants points toward exciton/SPP coupling as the root of the observed phenomena.[28]

When taken together, the experimental observations and simulations reveal a hybrid CTE/SPP system resulting from coupling between surface plasmons and the excitonic states in the PTCDA owing to the grating structure. The large absorptivity of PTCDA and the relatively narrow SPP produce a regime of coupling strong enough to render a clear change in photophysical observables, especially as a function of incident angle. Enhanced low-energy absorption, an attractive feature of similar systems, is predicted and may be observed experimentally at the low energy CT tail of the PTCDA/grating absorption spectrum, although it is not as strong as predicted by simulations (Figure S1 in the Supporting Information). Further work will be aimed at measuring the influence of such hybridization on the formation of free charge carriers across a donor−acceptor interface.

■ ASSOCIATED CONTENT

Ⓢ Supporting Information

Further information about spectral modeling, PTCDA film on glass reflectance spectrum, and full reflectance fits for all angles and samples. This material is available free of charge via the Internet at http://pubs.acs.org.

■ AUTHOR INFORMATION

Corresponding Author

*E-mail: justin.johnson@nrel.gov.

Notes

The authors declare no competing financial interest.

■ ACKNOWLEDGMENTS

This research was performed under a grant from the Laboratory Directed Research and Development program at the National Renewable Energy Laboratory, which is supported by the U.S. Department of Energy under Contract No. DE-AC36-08GO28308. W.P. acknowledges NSF CHE-1125935 grant. We thank Steve Christensen for assistance with atomic layer deposition and Zhen Wang and Yifu Ding for assistance with nanoimprint lithography.

■ REFERENCES

(1) Lee, J.; Vandewal, K.; Yost, S. R.; Bahlke, M. E.; Goris, L.; Baldo, M. A.; Manca, J. V.; Voorhis, T. V. Charge Transfer State Versus Hot Exciton Dissociation in Polymer−Fullerene Blended Solar Cells. *J. Am. Chem. Soc.* **2010**, *132*, 11878−11880.

(2) Clarke, T. M.; Durrant, J. R. Charge Photogeneration in Organic Solar Cells. *Chem. Rev.* **2010**, *110*, 6736−6767.

(3) Ohkita, H.; Cook, S.; Astuti, Y.; Duffy, W.; Tierney, S.; Zhang, W.; Heeney, M.; McCulloch, I.; Nelson, J.; Bradley, D. D. C.; Durrant, J. R. Charge Carrier Formation in Polythiophene/Fullerene Blend Films Studied by Transient Absorption Spectroscopy. *J. Am. Chem. Soc.* **2008**, *130*, 3030−3042.

(4) Smith, M. B.; Michl, J. Singlet Fission. *Chem. Rev.* **2010**, *110*, 6891−6936.

(5) Greyson, E. C.; Vura-Weis, J.; Michl, J.; Ratner, M. A. Maximizing Singlet Fission in Organic Dimers: Theoretical Investigation of Triplet

Yield in the Regime of Localized Excitation and Fast Coherent Electron Transfer. *J. Phys. Chem. B* **2010**, *114*, 14168−14177.
(6) Law, K. Y. Organic Photoconductive Materials: Recent Trends and Developments. *Chem. Rev.* **1993**, *93*, 449−486.
(7) Hains, A. W.; Liang, Z.; Woodhouse, M. A.; Gregg, B. A. Molecular Semiconductors in Organic Photovoltaic Cells. *Chem. Rev.* **2010**, *110*, 6689−6735.
(8) Li, C.; Wonneberger, H. Perylene Imides for Organic Photovoltaics: Yesterday, Today, and Tomorrow. *Adv. Mater.* **2012**, *24*, 613−636.
(9) Hoffmann, M.; Schmidt, K.; Fritz, T.; Hasche, T.; Agranovich, V. M.; Leo, K. The Lowest Energy Frenkel and Charge-Transfer Excitons in Quasi-One-Dimensional Structures: Application to Me-PTCDI and PTCDA Crystals. *Chem. Phys.* **2000**, *258*, 73−96.
(10) Bulović, V.; Burrows, P. E.; Forrest, S. R.; Cronin, J. A.; Thompson, M. E. Study of Localized and Extended Excitons in 3,4,9,10- Perylenetetracarboxylic Dianhydride (PTCDA) 0.1. Spectroscopic Properties of Thin Films and Solutions. *Chem. Phys.* **1996**, *210*, 1−12.
(11) Ferguson, A. J.; Jones, T. S. Photophysics of PTCDA and Me-PTCDI Thin Films: Effects of Growth Temperature. *J. Phys. Chem. B* **2006**, *110*, 6891−6898.
(12) Kobitski, A. Y.; Scholz, R.; Salvan, G.; Kampen, T. U.; Wagner, H. P.; Zahn, D. R. T. Time-Resolved Photoluminescence Study of Excitons in Thin PTCDA Films at Various Temperatures. *Appl. Surf. Sci.* **2003**, *212−213*, 428−432.
(13) Scholz, R.; Kobitski, A. Y.; Vragović, I.; Wagner, H. P.; Zahn, D. R. T. Time-Resolved Photoluminescence in α-PTCDA Single Crystals: Evidence for Recombination Via Frenkel Excitons, Charge Transfer States, and Excimers. *Org. Electron.* **2004**, *5*, 99−105.
(14) Scholz, R.; Schreiber, M.; Vragović, I.; Kobitski, A. Y.; Wagner, H. P.; Zahn, D. R. T. Influence of Exciton Transfer on the Optical Cycle of α-PTCDA. *J. Lumin.* **2004**, *108*, 121−126.
(15) Mobus, M.; Karl, N.; Kobayashi, T. Structure of Perylene-Tetracarboxylic-Dianhydride Thin-Films on Alkali-Halide Crystal Substrates. *J. Cryst. Growth* **1992**, *116*, 495−504.
(16) Heutz, S.; Ferguson, A. J.; Rumbles, G.; Jones, T. S. Morphology, Structure and Photophysics of Thin Films of Perylene-3,4,9,10-Tetracarboxylic Dianhydride. *Org. Electron.* **2002**, *3*, 119−127.
(17) Lovinger, A. J.; Forrest, S. R.; Kaplan, M. L.; Schmidt, P. H.; Venkatesan, T. Structural and Morphological Investigation of the Development of Electrical-Conductivity in Ion-Irradiated Thin-Films of an Organic Material. *J. Appl. Phys.* **1984**, *55*, 476−482.
(18) Cade, N. I.; Ritman-Meer, T.; Richards, D. Strong Coupling of Localized Plasmons and Molecular Excitons in Nanostructured Silver Films. *Phys. Rev. B* **2009**, *79*, 241404.
(19) Gomez, D. E.; Vernon, K. C.; Mulvaney, P.; Davis, T. J. Coherent Superposition of Exciton States in Quantum Dots Induced by Surface Plasmons. *Appl. Phys. Lett.* **2010**, *96*, 073108.
(20) Romero, M. J.; van de Lagemaat, J. Luminescence of Quantum Dots by Coupling with Nonradiative Surface Plasmon Modes in a Scanning Tunneling Microscope. *Phys. Rev. B* **2009**, *80*, 115432.
(21) Gan, Q. Q.; Bartoli, F. J.; Kafafi, Z. H. Plasmonic-Enhanced Organic Photovoltaics: Breaking the 10% Efficiency Barrier. *Adv. Mater.* **2013**, *25*, 2385−2396.
(22) Oskooi, A. F.; Roundy, D.; Ibanescu, M.; Bermel, P.; Joannopoulos, J. D.; Johnson, S. G. Meep: A Flexible Free-Software Package for Electromagnetic Simulations by the FDTD Method. *Comput. Phys. Commun.* **2010**, *181*, 687−702.
(23) Djurišić, A. B.; Fritz, T.; Leo, K. Modeling the Optical Constants of Organic Thin Films: Application to 3,4,9,10-Perylenetetracarboxylic Dianhydride (PTCDA). *Opt. Commun.* **2000**, *183*, 123−132.
(24) Johnson, P. B.; Christy, R. W. Optical Constants of Noble Metals. *Phys. Rev. B* **1972**, *6*, 4370−4379.
(25) Bellessa, J.; Bonnand, C.; Plenet, J. C.; Mugnier, J. Strong Coupling between Surface Plasmons and Excitons in an Organic Semiconductor. *Phys. Rev. Lett.* **2004**, *93*, 036404.
(26) Purcell, E. M. Spontaneous Emission Probabilities at Radio Frequencies. *Phys. Rev.* **1946**, *69*, 681.
(27) Anger, P.; Bharadwaj, P.; Novotny, L. Enhancement and Quenching of Single-Molecule Fluorescence. *Phys. Rev. Lett.* **2006**, *96*, 113002.
(28) Thomas, M.; Greffet, J. J.; Carminati, R.; Arias-Gonzalez, J. R. Single-Molecule Spontaneous Emission Close to Absorbing Nanostructures. *Appl. Phys. Lett.* **2004**, *85*, 3863−3865.